FAST AND ACCURATE ALGORITHM OF 3D MAGNETIC SURFACES RECONSTRUCTION IN STELLARATORS

V. Filippov[1], D. Grekov[1,2], V. Olefir[2]

[1]National Science Center "Kharkov Institute of Physics and Technology", Institute of Plasma Physics, Kharkiv, Ukraine;
[2]V.N. Karazin Kharkiv National University, Kharkiv, Ukraine

E-mail: grekov@ipp.kharkov.ua

An algorithm of calculation of approximating functions, which establish the one-to-one correspondence between the real coordinate mesh with arbitrary step and magnetic flux label in the whole plasma volume, was developed. It allows one to calculate flux label along the lines of sight of the applied diagnostics and to define the probes locations and RF antenna position in relation to the last closed magnetic surface. Moreover, now it is possible to provide fast visualization of magnetic configuration during the experiment.

PACS: 52.27.Ny

INTRODUCTION

Calculation of the specific vacuum magnetic configuration of "Uragan-2M" torsatron using Nemov's decomposition of magnetic field potentials [1] takes few minutes of PC processor time. Calculations with using Biot – Savart law [2] take even more time. The results of calculation of one configuration (60 toroidal cross-sections) occupy about 250 Mb of memory storage. On-line operation with such data arrays or calculation of magnetic configuration during the experiment is hardly possible. The principal objective of this work was to develop the algorithm of calculation of approximating functions, which establish the one-to-one correspondence between the real coordinate $\vec{r}$ mesh with arbitrary step and magnetic flux label ψ in the whole plasma volume.

1. THE ALGORITHM DESCRIPTION

Three coordinate systems which can be easily connected each other were used in this work. These coordinate systems are presented in Fig. 1.

The first coordinate system is the cylindrical one with the axis along the main axis of the torus (R,φ,Z) for initial calculations of magnetic field lines (Poincare plots).

The second coordinate system is the "quasicylindrical" one (ρ,φ,z), which is connected with the magnetic axis. It is necessary for intermediate calculations. Coordinates ρ and z are defined as

$$\rho = R - R_{axis}(\varphi), \quad z = Z - Z_{axis}(\varphi), \qquad (1)$$

here R_{axis} and Z_{axis} are coordinates of the magnetic axis.

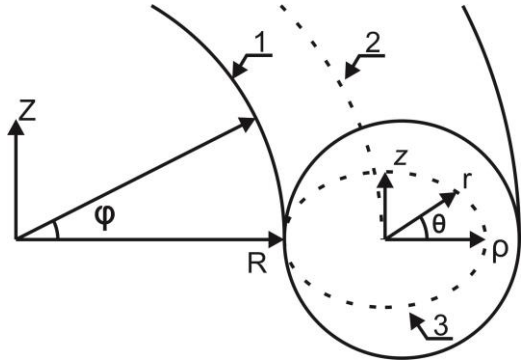

Fig. 1. Coordinate systems: 1 – vacuum vessel; 2 – magnetic axis; 3 – last closed magnetic surface (LCMS)

The third coordinate system (r,θ,φ) is quasitoroidal one, which is also connected with the magnetic axis

$$r = \sqrt{\rho^2 + z^2}, \quad \vartheta = \arctan(z/\rho). \qquad (2)$$

As an input parameters, L = 34 magnetic surfaces consisting of M = 400 poloidal points with N = 60 toroidal cross-sections were calculated using method [1] and used as example (Fig. 2). It should be noted that the values of the set *(L, M, N)* may vary. Also, the magnetic axis position in each of N cross-sections must be supplied. The dependencies of R_{axis} and Z_{axis} on toroidal angle φ are shown in Fig. 3. As can be clearly seen from this figure, these dependencies are perfectly approximated by series of the form

$$R_{axis}(\varphi) = \sum_0^S V_s \cos(4s\varphi), Z_{axis}(\varphi) = \sum_1^S W_s \sin(4s\varphi). \qquad (3)$$

The least squares method (LSA) was used to approximate V_s and W_s. As it turned out, the averaged approximation error was of the order of 10^{-9} cm at S = 7.

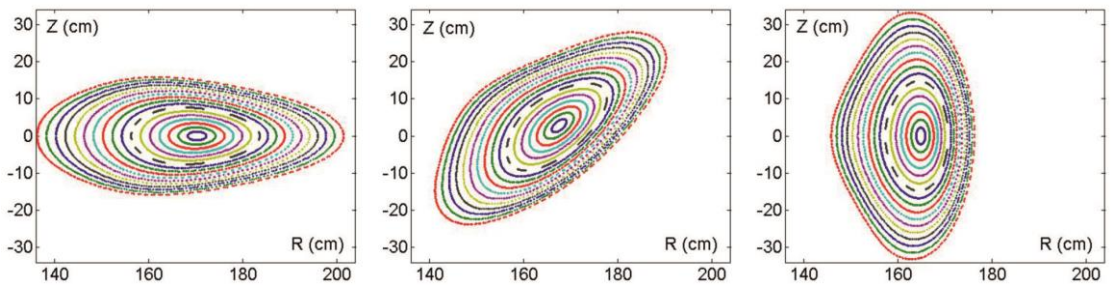

Fig. 2. Poincare plots in three toroidal cross-sections separated by $\Delta\varphi = \pi/8$

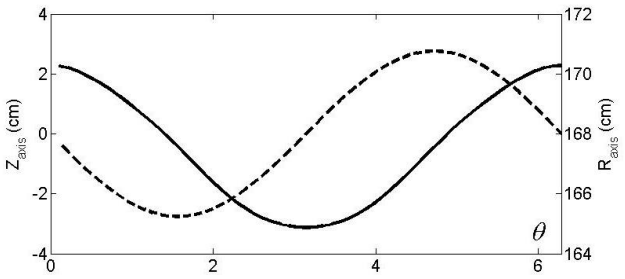

Fig. 3. Dependencies of R_{axis} (solid line) and Z_{axis} (dashed line) on toroidal angle

Hereinafter, each toroidal cross-section is indexed by n ($1 < n < N$). Each magnetic surface is indexed by l ($1 < l < L$). And each point at magnetic surface is indexed by m' ($1 < m' < M$). All subsequent actions relate to each magnetic surface and each toroidal cross-section.

Unfortunately, input data $R_{l,m',n}$ and $Z_{l,m',n}$ are distributed over magnetic surface irregularly in angle ϑ. This makes the accurate approximation of magnetic configuration impossible. In order to overcome this obstacle, it is necessary to rearrange input data. First, set $R_{l,m',n}$ and $Z_{l,m',n}$ was transformed into set $\rho_{l,m',n}$ and $z_{l,m',n}$. As it is seen from Fig. 4, $\rho_{l,m',n}$ and $z_{l,m',n}$ depend on m almost periodically. This motivated the expansion of $\rho_{l,m',n}$ and $z_{l,m',n}$ into trigonometric series over m. To this purpose, dependencies of $\vartheta_{l,n}$ on φ were established (Fig. 5) and coefficients of linear regressions $\omega_{l,n}$ were defined.

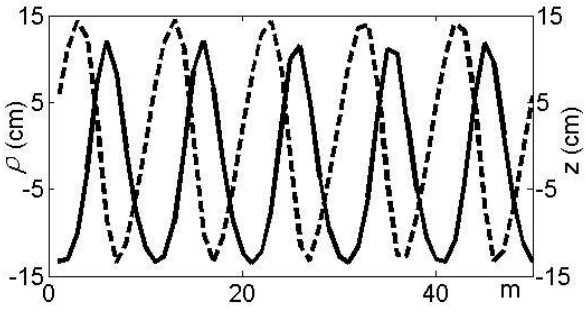

Fig. 4. Dependencies of $\rho_{15,m,17}$ (solid line) and $z_{15,m,17}$ (dashed line) on m

Finally, the values $\omega_{l,n}$ were averaged over the toroidal angle $\omega_l = \sum_1^N \omega_{l,n} / N$. These allowed to expand $\rho_{l,m',n}$ and $z_{l,m',n}$ into series

$$\rho_{l,n}(m') = \sum_{k=0}^{K} a_{l,n}^k \cos(m'\omega_l k) + \sum_{k=1}^{K} b_{l,n}^k \sin(m'\omega_l k),$$

$$z_{l,n}(m') = \sum_{k=0}^{K} c_{l,n}^k \cos(m'\omega_l k) + \sum_{k=1}^{K} d_{l,n}^k \sin(m'\omega_l k). \quad (4)$$

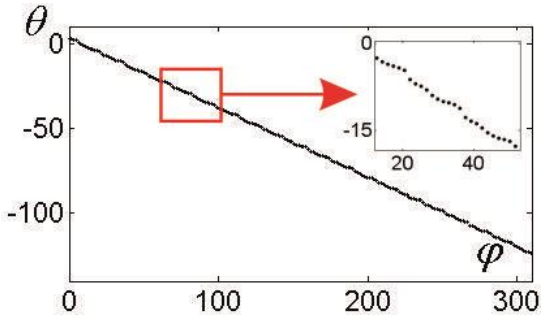

Fig. 5. Dependence of poloidal angle $\vartheta_{15,17}$ on toroidal angle φ

The value $K = 11$ was used to find coefficients by LSA. The error of LSA in this case was under 10^{-2} cm. Then these series were used in order to recalculate sets $\rho_{l,m,n}$ and $z_{l,m,n}$ at values ϑ_m, which are separated by constant step $\Delta\vartheta = 2\pi/M$. Values of $m'\omega_l$, corresponding to these ϑ_m, were calculated from Eqs. (2), (4) iteratively with relative error ~ 10^{-3}. New M = 128 was adopted and new poloidal index m = 1.2…128 K (Fig. 6).

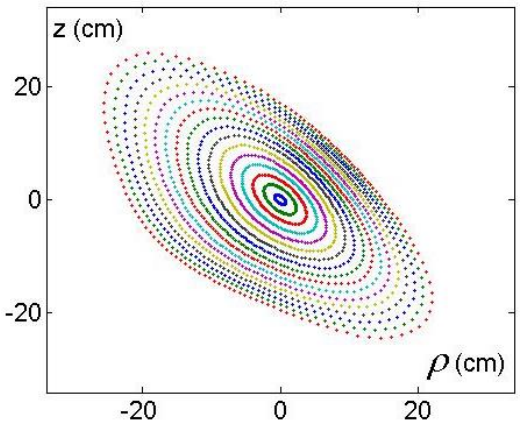

Fig. 6. New set of input data in toroidal cross-section n = 15

After that set $r_{l,m,n}$ was calculated using new $\rho_{l,m,n}$ and $z_{l,m,n}$. An averaged radius was calculated as $\bar{r}_l = \sum_{n=1}^{N}\sum_{m=1}^{M} r_{l,m,n} \Big/ (M \cdot N)$ and flux surface label ψ_l was defined as $\psi_l = \bar{r}_l / \bar{r}_L$. Such definition provide $\psi = 0$ at the magnetic axis and $\psi = 1$ at the LCMS.

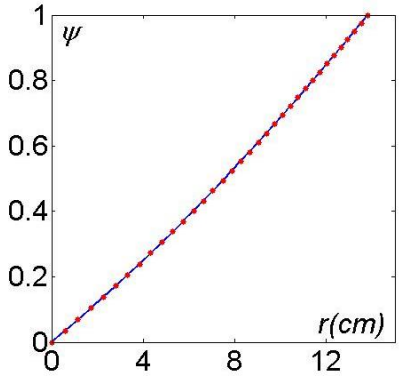

Fig. 7. Dependence of $\psi_{15,50}$ on r

Thus, on the rays, which started from magnetic axis in toroidal cross-section *n* in poloidal direction $m\Delta\vartheta$, the one-to-one correspondence established between $r_{m,n}$ and $\psi_{m,n}$: $r_{m,n} = r_{m,n}(\psi)$ and $\psi_{m,n} = \psi_{m,n}(r/a_c)$, where a_c is the vessel radius (see Fig. 7). This correspondence was approximated like

$$\psi_{m,n}(r/a_c) = \sum_{i=1}^{I} f^i_{m,n}(r/a_c)^i$$

and

$$r_{m,n}(\psi) = a_c \sum_{i=1}^{I} F^i_{m,n}\psi^i .$$

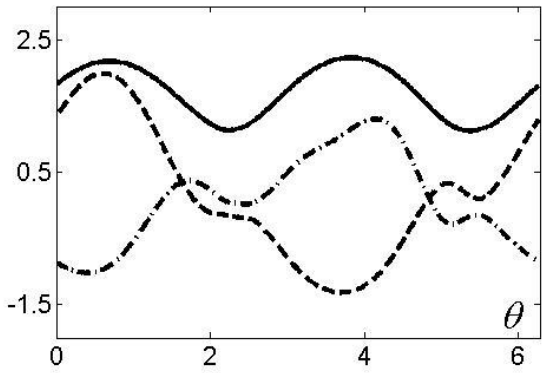

Fig. 8. Coefficients of polynomial decomposition of ψ vs poloidal angle for n = 15(f^1 – solid; f^2 – dashed; f^3 – dot and dashed lines)

As the calculations showed, $I = 3$ is sufficient for these representations (Fig. 8).

Then, coefficients $f^i_{m,n}$ (see Fig. 8) and $F^i_{m,n}$ were expanded into series over ϑ:

$$f^i_{m,n} = \sum_{j=0}^{J} g^{i,j}_n \cos(j\vartheta) + \sum_{j=1}^{J} \tilde{g}^{i,j}_n \sin(j\vartheta),$$

$$F^i_{m,n} = \sum_{j=0}^{J} G^{i,j}_n \cos(j\vartheta) + \sum_{j=1}^{J} \tilde{G}^{i,j}_n \sin(j\vartheta). \qquad (5)$$

At last, expansions over φ were fulfilled:

$$g^{i,j}(\varphi) = \sum_{k=0}^{K} h^{i,j,k} \cos(4k\varphi)$$

$$\tilde{g}^{i,j}(\varphi) = \sum_{k=1}^{K} \tilde{h}^{i,j,k} \sin(4k\varphi)$$

$$G^{i,j}(\varphi) = \sum_{k=0}^{K} H^{i,j,k} \cos(4k\varphi) \qquad (6)$$

$$\tilde{G}^{i,j}(\varphi) = \sum_{k=1}^{K} \tilde{H}^{i,j,k} \sin(4k\varphi)$$

In these expansions $J = 15$ and $K = 10$ were accepted. Combining together all expansions, following expressions were obtained Another verification of the accuracy of the approximation was carried out by calculating $\delta = \vec{B}\cdot\nabla\psi$. By definition, δ must be equal to zero. In fulfilled calculations, it is of the order of 10^{-3} (Fig. 10).

$$\psi_{m,n}(r/a_c,\theta,\varphi) = \sum_{i=1}^{I}\left(\sum_{j=0}^{J}\left[\sum_{k=0}^{K} h^{i,j,k}\cos(4k\varphi)\right]\cos(j\vartheta) + \sum_{j=1}^{J}\left[\sum_{k=1}^{K}\tilde{h}^{i,j,k}\sin(4k\varphi)\right]\sin(j\vartheta)\right)\cdot(r/a_c)^i ,$$

$$r_{m,n}(\psi,\theta,\varphi) = a_c\sum_{i=1}^{I}\left(\sum_{j=0}^{J}\left[\sum_{k=0}^{K} H^{i,j,k}\cos(4k\varphi)\right]\cos(j\vartheta) + \sum_{j=1}^{J}\left[\sum_{k=1}^{K}\tilde{H}^{i,j,k}\sin(4k\varphi)\right]\sin(j\vartheta)\right)\cdot(\psi)^i \quad . \qquad (7)$$

As the result, for the specific magnetic configuration $\psi(\vec{r})$ or $\vec{r}(\psi)$ completely defined by set of $I \cdot J \cdot K$ constants, which allow appropriate reconstructions during less then 1 s PC time.

2. VERIFICATION OF THE ALGORITHM

In order to check the accuracy of the proposed algorithm, the relative error in the calculations of $r_{m,n}(\psi)$ was defined for several values of *m* and *n*, see Fig. 9 for example. The relative error of calculations turned out to be less then 10^{-3}.

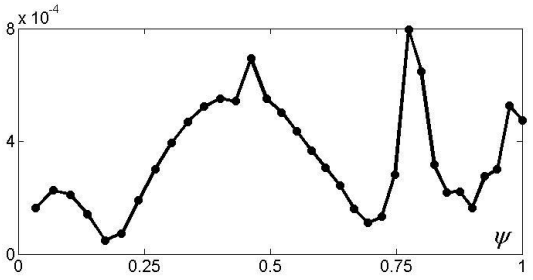

Fig. 9. The relative error of calculations of r

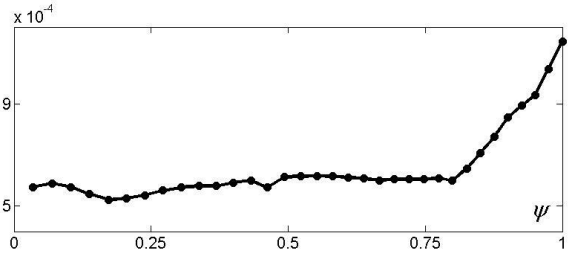

Fig. 10. The relative error in equality $\vec{B}\cdot\nabla\psi = 0$ for prescribed values of ψ

CONCLUSIONS

On an example of the U-2M torsatron it has been shown that application of the developed in this paper algorithm to the specific magnetic configuration allows one to define completely $\psi(r/a_c)$ or $r(\psi)$ by set of $I \cdot J \cdot K$ constants, which give appropriate reconstructions during less then 1 s PC time and occupy about 10 Kb of memory storage. The small volume of consumed memory gives the possibility to calculate in advance the decompositions of the big number of the

magnetic configurations. Then these decompositions may be used for:

- calculations of ψ along the along the lines of sight of the applied diagnostics;
- definition of probes locations and RF antenna position in relation to the last closed magnetic surface;
- procuring of the fast visualization of magnetic configuration;
- definition of local parameters in transport or wave codes, for example, in modeling of slow wave propagation in Wendelstein 7X.

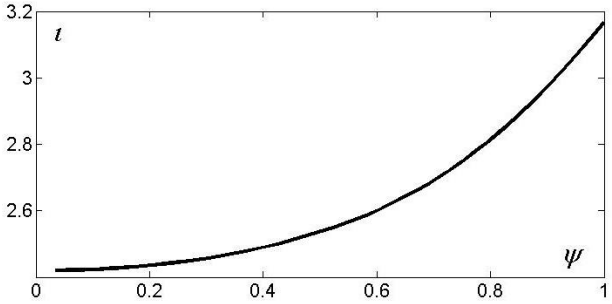

Fig. 11. Profile of the rotational transform

This algorithm may be used also for calculations of the input parameters – rotational transform profile (Fig. 11) and Furies decomposition of the LCMS - for VMEC code (Fig. 12).

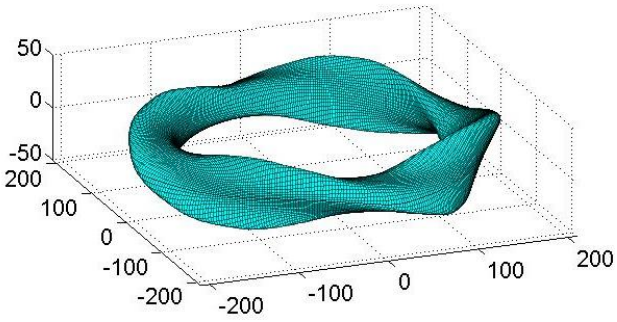

Fig. 12. Reconstructed LCMS of torsatron U-2M

ACKNOWLEDGEMENTS

This work has been carried out within the framework of the EUROfusion Consortium and has received funding from the Euratom research and training programme 2014-2018 under grant agreement No 633053. The views and opinions expressed herein do not necessarily reflect those of the European Commission.

REFERENCES

1. V.N. Kaljuzhnyj, V.V. Nemov // *Voprosy Atomnoj Nauki i Tekhn. Ser. "Termoyadern. Sintez"*. 1985, № 2, p. 35 (in Russian).
2. N.T. Besedin, G.G. Lesnyakov, I.M. Pankratov // *Voprosy Atomnoj Nauki i Tekhn. Ser. "Termoyadern. Sintez"*. 1991, № 1, p. 48 (in Russian).

Article received 02.10.2018

БЫСТРЫЙ И ТОЧНЫЙ АЛГОРИТМ ТРЕХМЕРНОЙ РЕКОНСТРУКЦИИ МАГНИТНЫХ ПОВЕРХНОСТЕЙ В СТЕЛЛАРАТОРАХ

В. Филиппов, Д. Греков, В. Олефир

Представлен быстрый и точный алгоритм вычисления аппроксимирующих функций, которые устанавливают взаимно однозначное соответствие между пространственными координатами в объеме плазмы и меткой магнитных поверхностей. С помощью этих функций можно вычислять значение метки магнитных поверхностей вдоль линий зондирования различных диагностик, определять положение зондов и позицию ВЧ-антенн относительно крайней замкнутой магнитной поверхности. Более того, стало возможным обеспечить быструю визуализацию магнитной конфигурации торсатрона во время проведения эксперимента.

ШВИДКИЙ ТА ТОЧНИЙ АЛГОРИТМ ТРИВИМІРНОЇ РЕКОНСТРУКЦІЇ МАГНІТНИХ ПОВЕРХОНЬ У СТЕЛАРАТОРАХ

В. Філіппов, Д. Греков, В. Олефір

Наведено швидкий та точний алгоритм обчислення функцій, що апроксимують магнітні поверхні торсатрона. Вони здійснюють взаємно однозначну відповідність між просторовими координатами в об'ємі плазми та позначкою магнітних поверхонь. За допомогою цих функцій можна обчислювати значення позначки магнітних поверхонь вздовж ліній зондування різних діагностик, визначати розташування зондів та положення ВЧ-антен відносно останньої замкнутої магнітної поверхні. Більш того, стає можливим забезпечити швидку візуалізацію магнітної конфігурації торсатрона під час проведення експерименту.